Time-resolved Vessel-selective Digital Subtraction MR Angiography of the Cerebral Vasculature with Arterial Spin Labeling[1]

Philip M. Robson, PhD
Weiying Dai, PhD
Ajit Shankaranarayanan, PhD
Neil M. Rofsky, MD
David C. Alsop, PhD

Purpose: To demonstrate an arterial spin-labeling (ASL) magnetic resonance (MR) angiographic technique that covers the entire cerebral vasculature and yields transparent-background, time-resolved hemodynamic, and vessel-specific information similar to that obtained with x-ray digital subtraction angiography (DSA) without the use of exogenous contrast agents.

Materials and Methods: Prior institutional review board approval and written informed consent were obtained for this HIPAA-compliant study in which 12 healthy volunteers (five women, seven men; age range, 21—62 years; average age, 28 years) underwent imaging. An ASL technique in which variable labeling durations are used to acquire hemodynamic inflow information and a vessel-selective pulsed-continuous ASL technique were tested. Region-of-interest signal intensities in various vessel segments were averaged across subjects and used to quantitatively compare images. For comparison, a standard time of flight (TOF) acquisition was performed in the circle of Willis.

Results: Inflow temporal resolution of 200 msec was demonstrated, revealing arterial transit times of 750, 950, and 1100 msec to consecutive segments of the middle cerebral artery from distal to the circle of Willis to deep regions of the midbrain. Selective labeling resulted in an average of eight-fold suppression of contralateral vessels relative to the labeled vessel. Signal-to-noise ratios and contrast-to-noise ratios on maximum intensity projection images obtained with 88-second volumetric acquisitions (60 ± 15 [standard deviation] and 57 ± 15, respectively) and 11-second single-projection acquisitions (19 ± 5 and 17 ± 5, respectively) were comparable with standard TOF acquisitions, in which a 2.7-fold longer imaging duration for a 2.6-fold lower pixel area was used. Normal variations of the vasculature were identified with ASL angiography.

Conclusion: ASL angiography can be used to acquire hemodynamic vessel-specific information similar to that obtained with x-ray DSA.

[1] From the Department of Radiology, Beth Israel Deaconess Medical Center and Harvard Medical School, 330 Brookline Ave, Ansin 242, Boston, MA 02215 (P.M.R., W.D., N.M.R., D.C.A.); and Global MR Applied Science Laboratory, GE Healthcare, Menlo Park, Calif (A.S.). Received December 18, 2009; revision requested February 10, 2010; revision received April 27; accepted May 13; final version accepted June 7. Supported by GE Healthcare, Waukesha, Wis. **Address correspondence to** P.M.R. (e-mail: *probson@bidmc.harvard.edu*).

Imaging of the cerebral vasculature is important in the diagnosis of many cerebrovascular diseases, including carotid artery stenosis (1), intracranial aneurysms, and arteriovenous malformations (2), as well as in the assessment of patients. Evaluation of hemodynamic function and identification of collateral circulation (3) are important in assessment of the risk of recurrent stroke or ischemia from occluded carotid arteries and in presurgical planning (2). X-ray digital subtraction angiography (DSA) is considered the reference standard for cerebral angiography (1–6), as it exhibits high spatial and temporal resolution of inflow dynamics and has the ability to selectively interrogate specific feeding vessels. However, this is an invasive procedure that is associated with morbidity and mortality (7–10).

The most popular magnetic resonance (MR) angiographic techniques used in clinical practice include time-of-flight (TOF) MR angiography (11), phase-contrast MR angiography (12), and dynamic contrast material–enhanced MR angiography (13). Dynamic contrast-enhanced MR angiography can be used to obtain high-spatial-resolution angiograms with varying degrees of temporal resolution (14). However, the attainable temporal resolution is ultimately limited by the width of the intravenous contrast material bolus. Hemodynamic information may also be inferred from the velocity data from phase-contrast MR angiography and the morphologic information from TOF MR angiography.

An alternative approach to MR angiography is arterial spin labeling (ASL) (15). Spin labeling is performed by inverting the magnetization of arterial water at a remote location outside the tissue of interest. After waiting an appropriate inflow time (the inversion time), an image of the tissue is acquired in which the signal of the tissue is modulated by the labeled blood that has flowed into the tissue. An angiographic image can be obtained with a short inversion time, with labeled signal still in the vessels. By using arterial water as an endogenous tracer, ASL is not restricted to a single pass, and since the blood can be labeled in the feeding artery with a selectable duration, the achievable temporal resolution is not constrained by intravenous bolus dynamics. Typically, ASL images are made by subtracting one labeled image from one control (unlabeled) image. The subtraction has the advantage of completely removing the background tissue signal. ASL has been proposed for MR angiographic applications in the cerebral vasculature and renal arteries (16–25). Furthermore, spin-labeling approaches have been used to assess hemodynamic function, including inflow in the vessels and arrival times to the tissue (26). Collateralization of flow within the cerebral vasculature has been investigated (27–29) by using labeling strategies that enable the user to distinguish between feeding vessels to allow mapping of perfusion territories in the brain (30–33). However, these studies have focused on smaller fields of view and limited portions of the vasculature, and researchers have not considered targeting specific vessels for angiography.

The purpose of this work was to demonstrate an ASL MR imaging angiographic technique that covers the entire cerebral vasculature and yields transparent-background, time-resolved hemodynamic, and vessel-specific information similar to that obtained with x-ray DSA, without the use of exogenous contrast agents.

Advance in Knowledge

- High-quality cerebral angiography covering the entire vasculature can be performed with an MR imaging technique that uses arterial spin-labeling (ASL) preparation and balanced steady-state free precession signal acquisition.

Implications for Patient Care

- This MR imaging method has the potential to aid in the assessment and monitoring of cerebral vasculature and hemodynamics in a similar manner to x-ray digital subtraction angiography, while avoiding exposure to exogenous contrast agents and ionizing radiation.
- Information regarding conditions exhibiting delayed arterial transit time and collateral flow pathways can be obtained noninvasively.

Materials and Methods

This study was supported in part by GE Healthcare (Waukesha, Wis) in the form of research funding and provision of equipment. One author (D.C.A.) receives research support from GE Healthcare. This author also is an inventor on a patent of the pulsed continuous ASL method used in this study, and he may receive royalties related to this patent in the future. Another author (A.S.) is an employee of GE Healthcare and had no control over data inclusion.

Prior institutional review board approval and written informed consent

Published online before print
10.1148/radiol.10092333

Radiology 2010; 257:507–515

Abbreviations:
ASL = arterial spin labeling
ATT = arterial transit time
BGS = background suppression
CNR = contrast-to-noise ratio
COW = circle of Willis
DSA = digital subtraction angiography
ICA = internal carotid artery
MCA = middle cerebral artery
MIP = maximum intensity projection
ROI = region of interest
SNR = signal-to-noise ratio
TOF = time of flight

Author contributions:
Guarantors of integrity of entire study, P.M.R., W.D., A.S., D.C.A.; study concepts/study design or data acquisition or data analysis/interpretation, all authors; manuscript drafting or manuscript revision for important intellectual content, all authors; manuscript final version approval, all authors; literature research, all authors; clinical studies, W.D., A.S.; statistical analysis, P.M.R., W.D., A.S.; and manuscript editing, all authors

Funding:
This research was supported by the National Institutes of Health, National Cancer Institute (grant CA121570) and the National Institute of Mental Health (grant MH080729).

See Materials and Methods for pertinent disclosures.

were obtained for this Health Insurance Portability and Accountability Act–compliant study in which two cohorts of six healthy volunteers (five women, seven men; age range, 21–62 years; average age, 28 years) underwent imaging. Healthy volunteers who had no contraindications to MR imaging and no recent health problems or surgery were recruited. No subjects were excluded.

ASL Strategy

ASL digital-subtraction MR angiography uses pulsed continuous ASL, as described in detail previously (34) (average applied radiofrequency field strength [B_1], 1.4 μT; average gradient strength, 0.7 mT/m; maximum gradient strength, 7 mT/m). Labeling is applied for up to 3 seconds; this period is sufficiently long for a continuous stream of labeled blood to advance into the vasculature of interest. Dynamic inflow is depicted by varying the duration of labeling prior to imaging. For each labeling duration, a time frame is acquired in which the leading edge of the labeled bolus has progressed further into the vasculature. Vessel-selective labeling (32,35–37) enables one to target a specific feeding vessel, analogous to catheter placement. We followed the method described by Dai et al (37) (average strength of gradient pulses was 1.5 mT/m, rotated in 15° increments).

Background suppression (BGS) (38,39) was used to reduce motion artifacts and avoid problems of receiver saturation or increased noise that can occur with large volumetric signal acquisition. BGS comprised selective presaturation pulses performed 3000 msec before imaging (four 10-msec 12.5-kHz quadrature-phase pulses performed 17 msec apart) followed by selective frequency-offset-corrected inversion pulses (C-shaped, 10.8-kHz bandwidth, 15.36 msec, $\beta = 509\ sec^{-1}$, $\mu = 6.2$; see definitions in Ordidge et al [40]). For dynamic inflow experiments (described later in this article), four pulses were performed 2401, 1358, 574, and 138 msec before imaging. For vessel-selective experiments, a trade-off between superior BGS and reduced signal loss from inefficiencies in the inversion pulses was made (38,41) in anticipation of less-efficient vessel-selective labeling. Three pulses were used, and they were performed 2065, 845, and 196 msec before imaging. Spatially selective BGS presaturation and inversion pulses were applied over the entire head, with the labeling plane positioned at the inferior edge of the selected region. When labeling, inflowing spins should be of opposite polarity to the tissue spins. To maintain correct labeling with BGS pulses performed during a long labeling period, labeling and control conditions were alternated after each successive BGS inversion pulse, as shown in Figure 1.

To ensure continued inflow of labeled blood during image acquisition, a pulsed ASL scheme was incorporated into the end of continuous labeling. This enabled us to label inflowing blood inferior to the labeling plane; this blood then flowed into the field of view after

Figure 1

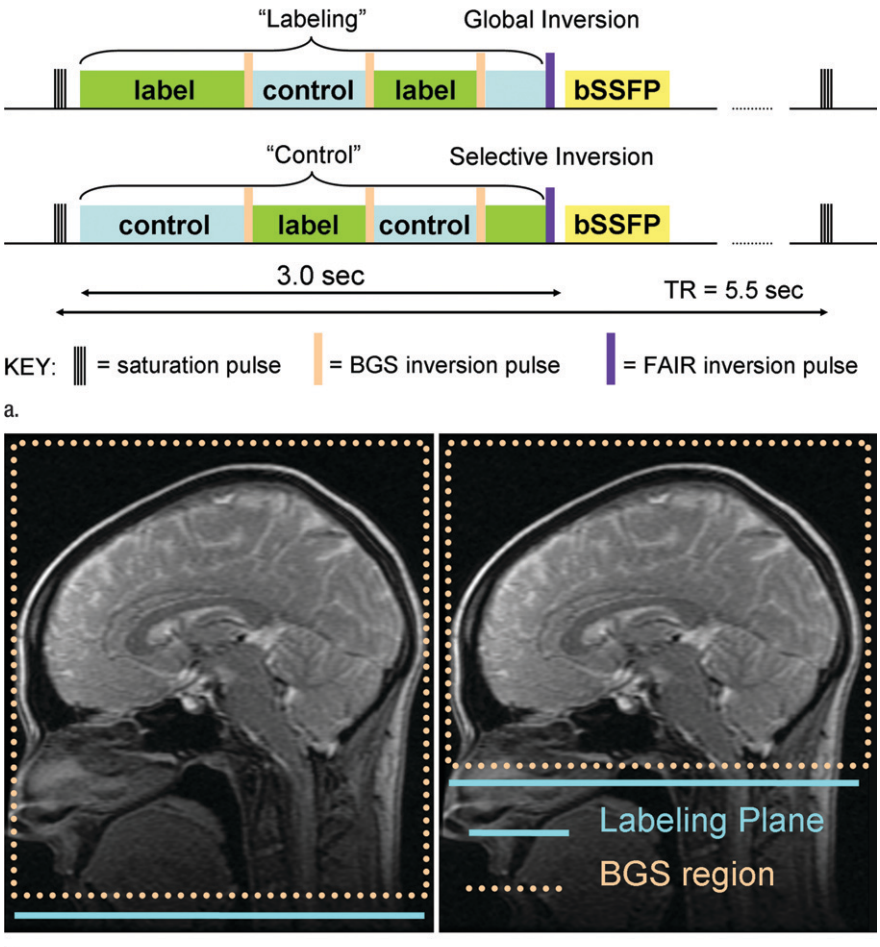

Figure 1: **(a)** Pulse sequence diagram shows interleaving of labeling and control conditions with BGS-selective (frequency-offset-corrected inversion) pulses is indicated. Alternating selectivity of flow-alternating inversion-recovery *(FAIR)* pulse used with nonselective labeling sequence is also shown. For selective labeling, only three BGS pulses with appropriately adjusted timing were used. *bSSFP* = balanced steady-state free precession sequence, *TR* = repetition time. **(b)** Labeling geometry (shown schematically on a locator image) indicates BGS region (boxes) and level of pulsed continuous ASL plane for inflow dynamic study and selective labeling of carotid arteries in cohort 2 (left). Note the more superior location for selective labeling in the internal carotid artery (ICA) above the carotid bifurcation in cohort 1 (right).

the end of continuous labeling. Spatial selectivity was alternated for the final BGS inversion pulse (nonselective for label conditions, selective for control conditions), as in the flow-alternating inversion-recovery labeling approach (42). No pulsed continuous ASL pulses were performed after the end of this inversion pulse; therefore, the shortest labeling time was 138 msec, with the final 138-msec period due to flow-alternating inversion-recovery–like labeling. Because of its global effect, the flow-alternating inversion-recovery pulse is not compatible with spatially targeted vessel-selective labeling and was not used.

Image Acquisition and Reconstruction

A balanced steady-state free precession (43) imaging module was used because of its well-known sensitivity to moving spins in blood as a result of inherent flow compensation. Hard 180° flip angle refocusing pulses were used to prevent recovery during the echo train of background tissue signal maintaining BGS, provide signal stability, and prevent spin dephasing. A half-angle pulse and five dummy pulses were used to allow signal instability to subside. Imaging parameters were as follows: repetition time msec/echo time msec, 4.4/2.2; 83-kHz receiver bandwidth; 256 × 256 matrix, 24-cm field of view; partial Fourier factor, 9/16; all echoes per section encode in one excitation after one spin preparation; and 5.5-second repetition time between spin preparation cycles. Most acquisitions were performed with eight section encodes (36-mm section thickness, 1.5-minute acquisition); however, single-projection images that required only 11 seconds to obtain were also acquired to enable us to assess the feasibility of faster acquisition. Complex images were subtracted before final display as maximum intensity projection (MIP) images.

Experiments

A 1.5-T MR imager (Excite HDx; GE Healthcare) and an eight-channel phased array-receiver head coil were used in this study.

Images of dynamic inflow at the level of the common carotid arteries were obtained with successive acquisitions with labeling durations of 138, 200, 400, 600, 800, 1000, 1200, 1400, 1600, 2000, and 2500 msec. Vessel-selective labeling was then investigated. A labeling duration of 2000 msec was used. An equivalent non–vessel-selective image was also acquired, with labeling applied at the same craniocaudal level. In the first cohort, imaging was focused on the cerebral arteries above the circle of Willis (COW), labeling in a segment of the ICA that was approximately straight, approximately halfway between the COW and the carotid bifurcation. In the second cohort, the extracranial carotid arteries were imaged, labeling in a segment of the common carotid arteries, 140 mm below the image center (Fig 1).

In the first cohort, a standard three-dimensional TOF MR angiogram centered on the COW was acquired in the axial orientation with the following parameters: 41/2.9; field of view, 23 × 17.25 cm; matrix, 320 × 192; 40 sections acquired; 1.6-mm section thickness reconstructed to 0.8 mm; flip angle, 20°; bandwidth, 31.25 kHz; and examination time, 4 minutes. For vessel location in both cohorts, an additional three-dimensional TOF sequence was performed. For this sequence, the field of view was positioned over the carotid vessels in the neck, and the same imaging parameters were used, albeit with a thicker 2.4-mm section. The whole session lasted approximately 1 hour.

Image Assessment

One author (P.M.R.; 4 years of experience, familiar with the anatomic structures studied herein) who was not blinded to image acquisition data performed all image analysis. For dynamic inflow measurements, regions of interest (ROIs) were placed on the MIP images at multiple locations, as shown in Figure 2. For selectivity measurements, ROIs were selected at similar positions on the left and right sides. ROIs were approximately 20–40 mm^2. They were selected manually and placed at locations that could be easily and consistently accessed across all subjects. Each location was approximately a constant distance from the COW and the labeling plane. ROIs were selected once on the images acquired with nonselective labeling applied for 2000 msec and used for all preceding time points or selectively labeled images, thereby preventing reader bias.

For inflow measurements, average signal was plotted against labeling duration; data were temporally smoothed by averaging neighboring points, and twofold linear interpolation was performed. The arterial transit time (ATT) was measured as the labeling duration for the signal to reach more than half of its final value. (ATT included the labeling duration plus the interval between the start of acquisition and the center of k-space acquisition [70.4 msec].) This value was averaged across all subjects in each cohort for each vessel segment.

For labeling selectivity measurements, to account for biasing of the small signal in contralateral vessels due to noise on these magnitude signal combined MIP images, we used a nonlinear intensity correction that was based on the probability distribution of magnitude signals in an MIP through eight sections, with use of the magnitude noise statistics described by Constantinides and colleagues (44). The ratio of contralateral to ipsilateral signal was plotted and averaged across subjects. In addition, ratio of the basilar artery to the ipsilateral proximal MCA segment in cohort 1 (cerebral vessels) and ratio of the ipsilateral vertebral artery to the proximal MCA segment in cohort 2 (carotid vessels) were found and averaged across subjects in respective cohorts.

Signal-to-noise ratio (SNR) and contrast-to-noise ratio (CNR) were measured from the average signal in ROIs placed on the carotid arteries inferior to the COW and the background tissue, as well as from the standard deviation of an ROI in the background air with the following equations: SNR = V/N, where V represents vessel and N represents noise, and CNR = $(V-T)/N$, where T represents tissue. Noise biases were corrected. Measurements were obtained from MIP images derived from

Figure 2

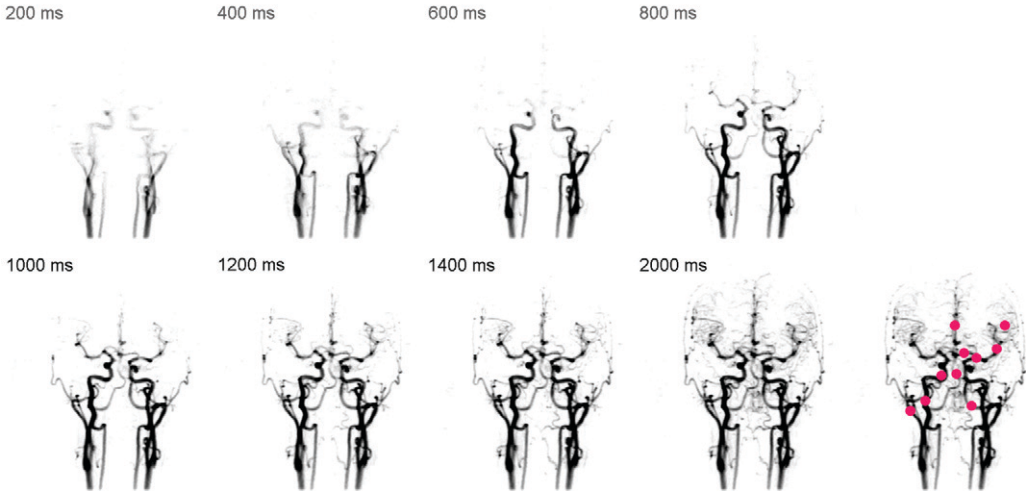

Figure 2: Coronal MIP images show time-resolved inflow dynamics. Filling of vasculature can be seen on each frame, with progressive durations of spin labeling prior to image acquisition. No delayed or asymmetric filling was observed. ROIs used in quantitative analysis are shown in red on the bottom right image. Certain segments (Table 1) progress distally from the COW.

eight section-encoding acquisitions, single-projection images with nonselective labeling applied for 2000 msec, and MIP images of the COW obtained with TOF MR angiography in cohort 1.

Statistical Analyses

For dynamic inflow measurements, one-sided paired *t* tests were used to determine whether arterial arrival time in a distal segment was later than arterial arrival time in a more proximal segment. ATT values were averaged over subjects in each cohort and compared. For selectivity measurements, two-sided single-sample *t* tests were used to determine whether the average ratio of contralateral-to-ipsilateral signal took a value different from 1 (the latter indicates no difference in the signal in equivalent vessels on opposing sides). ROI signal values were compared, with averaging over subjects in the respective cohort. In general, statistical significance was defined as $P < .05$. We used commercially available software (Microsoft Excel 2003 SP3; Microsoft, Seattle, Wash) to perform the analysis.

Results

Time-resolved images of the extracranial carotid arteries are shown in Figure 2; these images were acquired with a temporal resolution of 200 msec, and eight time frames are shown, with labeling durations of 200, 400, 600, 800, 1000, 1200, 1400, and 2000 msec. This time series of eight labeling durations required 12 minutes to acquire; however, this could be reduced to 1.5 minutes with single-projection acquisitions. Average ATTs obtained from dynamic inflow measurements are summarized in Table 1 for a variety of vessel segments in each hemisphere in cohorts 1 and 2. Progressively later arrival times to more distal segments are observed, as would be expected. Significant differences ($P < .04$) in arrival times were found between the COW and the various cerebral vessel segments (Table 1). Furthermore, additional significant differences were found between various pairs of proximal and distal vessel segments (Table 1). In cohort 1, labeling in the internal carotid artery, values of ATT averaged across hemispheres were 750, 950, and 1100 msec for consecutive segments of the middle cerebral artery from immediately distal to the COW to deep regions of the midbrain; this finding was in agreement with findings reported in the literature (20).

MIP images that show labeling targeted to the left common carotid artery and ICA are shown in Figure 3. These images, which cover the entire cerebral vasculature in projection format and with a transparent background, are similar to images acquired with x-ray DSA. Coronal and sagittal MIPs were reconstructed from separate acquisitions. Measurements from the vessel-selective labeling experiments are summarized in Table 2. We found a high degree of vessel selectivity. An average of eightfold suppression of contralateral vessels relative to the labeled vessel was achieved; the residual signal in the contralateral vessel was 0.12 ± 0.07 of the signal in the (ipsilateral) labeled vessel. Ratios for all vessel segments were significantly different from a value of 1 ($P < .001$), as shown in Table 2. Average ratios of the basilar artery (cohort 1) and ipsilateral vertebral artery (cohort 2) to the ipsilateral proximal MCA segment were 0.05 ± 0.02 and 0.41 ± 0.40, respectively, and showed significant contralateral signal suppression ($P < .001$ and $P = .014$, respectively). The ratio of 0.41 in the ipsilateral vertebral artery indicates that there can be substantial residual partial labeling of nearby vessels. The appearance of the trailing edge in the carotid arteries in Figure 3 highlights the benefit of using the flow-alternating inversion-recovery pulse at the end of labeling. This pulse was not used for vessel-selective acquisition.

In some volunteers, normal variations of the vasculature were observed. In these subjects, visualization and dynamic and selective assessment of the

Table 1

ATTs to Various Vessel Segments

Cohort and Segment	ATT (msec)
Cohort 1	
Below COW, left	<500*
ACA_a, left	850 ± 164
MCA_a, left	750 ± 148†
MCA_b, left	990 ± 148‡
MCA_c, left	1110 ± 423‡
ECA, left	650 ± 130
ACA_b	990 ± 84§
Below COW, right	<500*
ACA_a, right	650 ± 179‖
MCA_a, right	750 ± 179#
MCA_b, right	910 ± 55‡
MCA_c, right	1090 ± 398‡
ECA, right	650 ± 130
Basilar	890 ± 84
Cohort 2	
Carotid, above bifurcation, left	408 ± 97
Carotid, below COW, left	491 ± 166
ECA, left	441 ± 131
Vertebral, left	812 ± 301††
MCA_a, left	820 ± 187**
Basilar	1037 ± 103
Carotid, above bifurcation, right	395 ± 107
Carotid, below COW, right	487 ± 147
ECA, right	462 ± 262
Vertebral, right	854 ± 117‡‡
MCA_a, right	804 ± 207**
ACA_b	987 ± 116**

Note.—Unless otherwise indicated, data are mean ATTs ± standard deviations. Mean ATT was defined as the labeling duration at which ROI signal was greater than one-half of its value with 2.5 seconds of labeling. Standard deviation was calculated across subjects in each cohort. ATT included time to acquisition of the center of k-space. Significant differences in ATT were found between various segments (left and right branches were assessed separately) with the one-sided paired *t* test. In cohort 1, $P < .01$ for all MCA and ACA branches compared to the COW, unless otherwise indicated. ACA = anterior cerebral artery, ECA = external carotid artery, MCA = middle cerebral artery. Subscripts a, b, and c indicate relative distance along the artery from the COW, with a being the closest.

* Data are mean ATTs.

† $P = .03$.

‡ $P < .04$ in comparison with MCA_a.

§ From ACA_a to ACA_b, $P = .07$ for left and $P = .005$ for right.

‖ $P = .19$.

$P = .04$.

** $P < .014$ between the COW and MCA/ACA branches.

†† $P = .07$ between vertebral and basilar arteries.

‡‡ $P = .014$ between vertebral and basilar arteries.

Figure 3

Figure 3: MIP images acquired with vessel-selective labeling (left column) and nonselective labeling (right column) at the same craniocaudal level in the common carotid artery (top row) and ICA (bottom row). Coronal (top row) and sagittal (bottom row) images were obtained with separate acquisitions. Excellent suppression of contralateral vessels and posterior circulation are shown in coronal and sagittal images, respectively. In all images, labeling plane is located at lower edge of image.

Table 2

Vessel Selectivity Measurements

Segment and Cohort	Ratio
Cohort 1	
ACA left	0.19 ± 0.09
MCA_a left	0.08 ± 0.05
MCA_b left	0.07 ± 0.04
MCA_c left	0.08 ± 0.03
Average	0.10 ± 0.07
Cohort 2	
Carotid– above bifurcation	0.14 ± 0.06
Carotid– below COW	0.16 ± 0.06
ECA	0.12 ± 0.06
MCA_a	0.13 ± 0.05
Average	0.14 ± 0.06
Average for all segments	0.12 ± 0.07

Note.—Data are means ± standard deviations. Selectivity was measured as the ratio of signal in vessel segments in hemispheres contralateral and ipsilateral to selective labeling in the ICA. ROI values were averaged across subjects. A high degree of selectivity is shown: All ratios are significantly different from a value of 1 ($P < .001$), where a value of 1 represents nonselectivity. ACA = anterior cerebral artery, ECA = external carotid artery. Subscripts a, b, and c indicate relative distance along the artery from the COW, with a being the closest.

vasculature with ASL digital subtraction MR angiography were consistent with anatomic findings of TOF MR angiography (Fig 4).

The overall quality of ASL digital subtraction MR angiography can be seen in Figure 5, where labeling for 2000 msec has filled the entire cerebral vasculature. The average SNR (mean ± SD across all subjects' left and right ICAs) of 60 ± 15 shows the high quality of the MIP images. The average CNR was 57 ± 15, which indicates the high degree of subtraction attained with the BGS. Equivalent values of SNR and CNR from TOF MR angiography of the COW were 34 ± 2 and 19 ± 2, respectively, indicating that the two techniques offer a similar and acceptable level of SNR. However, given the differences in image resolution and examination time, it should be noted that SNR comparison is not a definitive comparison in that it cannot account for the additional benefits of the ASL and TOF techniques. Projection images acquired in 11 seconds (Fig 5) show the major cerebral vessels with a decline in image quality compared with the image acquired with section encoding (Fig 5); this decline was primarily due to loss in SNR in proportion to the square root of acquisition time. Average SNR and CNR values were 19 ± 5 and 17 ± 5, respectively.

Figure 4

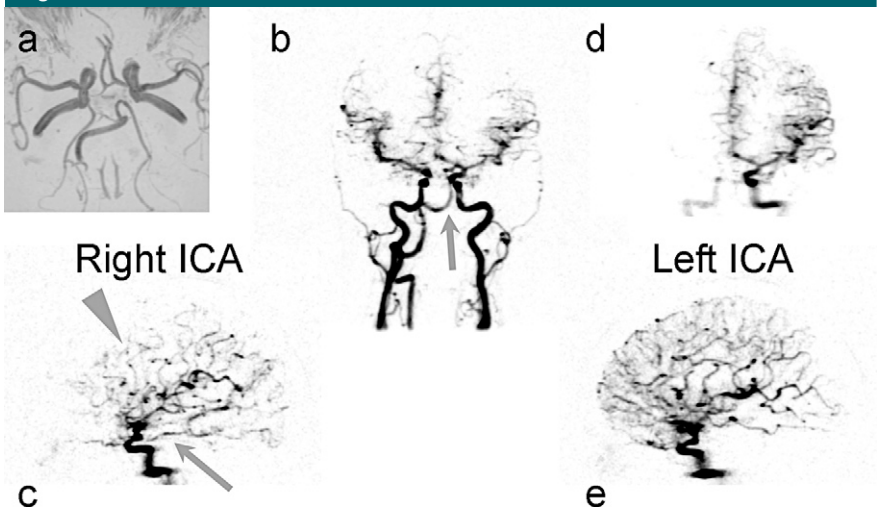

Figure 4: **(a)** Axial TOF MIP image of the COW enabled us to confirm normal anatomic variation identified with ASL digital-subtraction MR angiography. **(b)** Coronal eight-section ASL MIP image obtained with nonselective labeling shows weakly flowing left vertebral artery and right vertebral artery filling the basilar artery, which then appears directed toward left hemisphere (arrow). **(c)** Sagittal eight-section ASL MIP image obtained with labeling in right ICA shows feeding into posterior circulation (arrow) and diminished flow into anterior territory (arrowhead). **(d)** Coronal and **(e)** sagittal eight-section ASL MIP images obtained with labeling in left ICA show flow into both anterior cerebral branches.

Figure 5

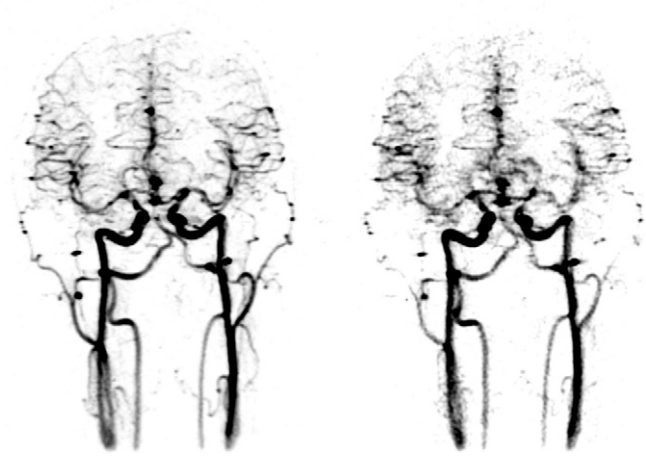

Figure 5: Left: Coronal MIP image obtained with eight-section-encoding 3D acquisition and imaging time of 1.5 minutes. Right: Coronal single-projection image acquired in 11 seconds.

Discussion

By using various labeling durations and endogenous water as the tracer, ASL is—in principle—not restricted in temporal resolution, unlike dynamic contrast-enhanced MR angiographic methods, which are restricted in temporal resolution; this finding makes 50-msec temporal resolution comparable to that used for x-ray DSA (45) feasible. However, the examination time needed to acquire multiple images at finer temporal resolution may become prohibitive, and spreading out of the bolus or pulsatility effects may blur temporal resolution. In some instances, temporal resolution greater than the 200 msec resolution shown here in healthy subjects may be required (21). With ASL, inflow sensitivity is determined by magnetization preparation—allowing flexibility in signal acquisition (acquisition of a wide field of view)—or by refocusing pulse trains, which may reduce sensitivity to dephasing around stenoses, as occurs with TOF MR angiography and phase-contrast MR angiography. Rapid projection imaging is possible with this technique and enables one to avoid the long examination times associated with phase-contrast MR angiography and TOF MR angiography.

This study was limited by the small number of subjects. The fact that we included only healthy volunteers meant that we could not investigate delayed ATTs or compare this technique with dynamic contrast-enhanced techniques. The principal limitation was the potential partial labeling of vessels in close proximity to the vessel-selective labeling site (37). This is particularly important if labeling is to be performed in the vertebral arteries where flow is low and contamination from partial labeling of the nearby carotid vessels may dominate. Second, the T1 decay of the label may limit the extent to which slow inflow can be imaged. Third, movement of the leading edge of the bolus of labeled blood during acquisition and the effect of pulsatility on the definition of the leading edge of the bolus have the potential to blur the image. Cardiac gating and additional averaging over the cardiac cycle may yield improvements. Fourth, small signal variations within vessels seen in Figures 2–5 are potentially problematic in relation to diagnosis of partial stenosis. Technical improvements in the selective labeling and acquisition are expected to improve vessel specificity and overall image quality.

ASL is not hampered by choosing an appropriate velocity encoding coefficient, as in phase-contrast MR angiography. As kinetic models show (46), continuous ASL is not hampered by the choice of inversion time. Steady-state peak signal is attained with continuous ASL with long labeling times. This enables one to acquire the maximal signal after a labeling time that need not depend on the blood transit time, whereas, in pulsed ASL, the inversion time required to attain peak signal is determined by the transit delay. Together with the

sensitivity advantage of continuous ASL, this is important in the presence of complicated flow where long and/or variable transit delays or collateral pathways may be present in patients with cardiovascular disease. Furthermore, pulsed ASL angiographic approaches that do not involve subtraction (16) rely on setting inversion time to attain BGS. Without exposure to ionizing radiation or exogenous contrast agents, this technique is particularly suited to screening or longitudinal evaluations. This study shows that MR imaging and ASL can be used to perform cerebral angiography with dynamic inflow and vessel-specific information that is similar to that obtained with conventional x-ray DSA. The combination of such attributes will be valuable as a complement to high-spatial-resolution anatomic MR angiography and high-temporal-resolution dynamic contrast-enhanced MR angiography (47).

References

1. Borisch I, Horn M, Butz B, et al. Preoperative evaluation of carotid artery stenosis: comparison of contrast-enhanced MR angiography and duplex sonography with digital subtraction angiography. AJNR Am J Neuroradiol 2003;24(6):1117–1122.
2. Anzalone N, Scomazzoni F, Strada L, Patay Z, Scotti G. Intracranial vascular malformations. Eur Radiol 1998;8(5):685–690.
3. Awad I, Little JR, Modic MT, Furlan AJ. Intravenous digital subtraction angiography: an index of collateral cerebral blood flow in internal carotid artery occlusion. Stroke 1982;13(4):469–472.
4. Endarterectomy for moderate symptomatic carotid stenosis: interim results from the MRC European Carotid Surgery Trial. Lancet 1996;347(9015):1591–1593.
5. Executive Committee for the Asymptomatic Carotid Atherosclerosis Study. Endarterectomy for asymptomatic carotid artery stenosis. JAMA 1995;273(18):1421–1428.
6. North American Symptomatic Carotid Endarterectomy Trial Collaborators. Beneficial effect of carotid endarterectomy in symptomatic patients with high-grade carotid stenosis. N Engl J Med 1991;325(7):445–453.
7. Heiserman JE, Dean BL, Hodak JA, et al. Neurologic complications of cerebral angiography. AJNR Am J Neuroradiol 1994;15(8):1401–1407; discussion 1408–1411.
8. Grzyska U, Freitag J, Zeumer H. Selective cerebral intraarterial DSA: complication rate and control of risk factors. Neuroradiology 1990;32(4):296–299.
9. Waugh JR, Sacharias N. Arteriographic complications in the DSA era. Radiology 1992;182(1):243–246.
10. Leffers AM, Wagner A. Neurologic complications of cerebral angiography: a retrospective study of complication rate and patient risk factors. Acta Radiol 2000;41(3):204–210.
11. Dumoulin CL, Cline HE, Souza SP, Wagle WA, Walker MF. Three-dimensional time-of-flight magnetic resonance angiography using spin saturation. Magn Reson Med 1989;11(1):35–46.
12. Bryant DJ, Payne JA, Firmin DN, Longmore DB. Measurement of flow with NMR imaging using a gradient pulse and phase difference technique. J Comput Assist Tomogr 1984;8(4):588–593.
13. Warach S, Li W, Ronthal M, Edelman RR. Acute cerebral ischemia: evaluation with dynamic contrast-enhanced MR imaging and MR angiography. Radiology 1992;182(1):41–47.
14. Korosec FR, Frayne R, Grist TM, Mistretta CA. Time-resolved contrast-enhanced 3D MR angiography. Magn Reson Med 1996;36(3):345–351.
15. Golay X, Hendrikse J, Lim TC. Perfusion imaging using arterial spin labeling. Top Magn Reson Imaging 2004;15(1):10–27.
16. Kanazawa H, Miyazaki M. Time-spatial labeling inversion tag (t-SLIT) using a selective IR-tag on/off pulse in 2D and 3D half-Fourier FSE as arterial spin labeling [abstr]. In: Proceedings of the Tenth Meeting of the International Society for Magnetic Resonance in Medicine. Berkeley, Calif: International Society for Magnetic Resonance in Medicine, 2002; 140.
17. Dixon WT, Du LN, Faul DD, Gado M, Rossnick S. Projection angiograms of blood labeled by adiabatic fast passage. Magn Reson Med 1986;3(3):454–462.
18. Edelman RR, Siewert B, Adamis M, Gaa J, Laub G, Wielopolski P. Signal targeting with alternating radiofrequency (STAR) sequences: application to MR angiography. Magn Reson Med 1994;31(2):233–238.
19. Günther M, Bock M, Schad LR. Arterial spin labeling in combination with a look-locker sampling strategy: inflow turbo-sampling EPI-FAIR (ITS-FAIR). Magn Reson Med 2001;46(5):974–984.
20. Warmuth C, Rüping M, Förschler A, et al. Dynamic spin labeling angiography in extracranial carotid artery stenosis. AJNR Am J Neuroradiol 2005;26(5):1035–1043.
21. Sallustio F, Kern R, Günther M, et al. Assessment of intracranial collateral flow by using dynamic arterial spin labeling MRA and transcranial color-coded duplex ultrasound. Stroke 2008;39(6):1894–1897.
22. Miyazaki M, Sugiura S, Tateishi F, Wada H, Kassai Y, Abe H. Non-contrast-enhanced MR angiography using 3D ECG-synchronized half-Fourier fast spin echo. J Magn Reson Imaging 2000;12(5):776–783.
23. Satogami N, Okada T, Koyama T, Gotoh K, Kamae T, Togashi K. Visualization of external carotid artery and its branches: non-contrast-enhanced MR angiography using balanced steady-state free-precession sequence and a time-spatial labeling inversion pulse. J Magn Reson Imaging 2009;30(3):678–683.
24. Nishimura DG, Macovski A, Pauly JM, Conolly SM. MR angiography by selective inversion recovery. Magn Reson Med 1987;4(2):193–202.
25. Roberts DA, Bolinger L, Detre JA, Insko EK, Bergey P, Leigh JS Jr. Continuous inversion angiography. Magn Reson Med 1993;29(5):631–636.
26. Hendrikse J, van Osch MJ, Rutgers DR, et al. Internal carotid artery occlusion assessed at pulsed arterial spin-labeling perfusion MR imaging at multiple delay times. Radiology 2004;233(3):899–904.
27. Taoka T, Iwasaki S, Nakagawa H, et al. Distinguishing between anterior cerebral artery and middle cerebral artery perfusion by color-coded perfusion direction mapping with arterial spin labeling. AJNR Am J Neuroradiol 2004;25(2):248–251.
28. van Laar PJ, van der Grond J, Bremmer JP, Klijn CJ, Hendrikse J. Assessment of the contribution of the external carotid artery to brain perfusion in patients with internal carotid artery occlusion. Stroke 2008;39(11):3003–3008.
29. Chng SM, Petersen ET, Zimine I, Sitoh YY, Lim CC, Golay X. Territorial arterial spin labeling in the assessment of collateral circulation: comparison with digital subtraction angiography. Stroke 2008;39(12):3248–3254.
30. Hendrikse J, van der Grond J, Lu H, van Zijl PC, Golay X. Flow territory mapping of the cerebral arteries with regional perfusion MRI. Stroke 2004;35(4):882–887.
31. Golay X, Petersen ET, Hui F. Pulsed star labeling of arterial regions (PULSAR): a robust

regional perfusion technique for high field imaging. Magn Reson Med 2005;53(1):15–21.

32. Werner R, Norris DG, Alfke K, Mehdorn HM, Jansen O. Continuous artery-selective spin labeling (CASSL). Magn Reson Med 2005; 53(5):1006–1012.

33. Günther M. Efficient visualization of vascular territories in the human brain by cycled arterial spin labeling MRI. Magn Reson Med 2006;56(3):671–675.

34. Dai W, Garcia D, de Bazelaire C, Alsop DC. Continuous flow-driven inversion for arterial spin labeling using pulsed radio frequency and gradient fields. Magn Reson Med 2008; 60(6):1488–1497.

35. Kansagra AP, Wong EC. Quantitative assessment of mixed cerebral vascular territory supply with vessel encoded arterial spin labeling MRI. Stroke 2008;39(11): 2980–2985.

36. Wong EC. Vessel-encoded arterial spin-labeling using pseudocontinuous tagging. Magn Reson Med 2007;58(6):1086–1091.

37. Dai W, Robson P, Shankaranarayanan A, Alsop D. Modified pulsed-continuous arterial spin labeling for labeling of a single artery. Magn Reson Med (in press).

38. Robson PM, Madhuranthakam AJ, Dai W, Pedrosa I, Rofsky NM, Alsop DC. Strategies for reducing respiratory motion artifacts in renal perfusion imaging with arterial spin labeling. Magn Reson Med 2009;61(6): 1374–1387.

39. Dixon WT, Sardashti M, Castillo M, Stomp GP. Multiple inversion recovery reduces static tissue signal in angiograms. Magn Reson Med 1991;18(2):257–268.

40. Ordidge RJ, Wylezinska M, Hugg JW, Butterworth E, Franconi F. Frequency offset corrected inversion (FOCI) pulses for use in localized spectroscopy. Magn Reson Med 1996;36(4):562–566.

41. Garcia DM, Duhamel G, Alsop DC. Efficiency of inversion pulses for background suppressed arterial spin labeling. Magn Reson Med 2005;54(2):366–372.

42. Kim SG. Quantification of relative cerebral blood flow change by flow-sensitive alternating inversion recovery (FAIR) technique: application to functional mapping. Magn Reson Med 1995;34(3):293–301.

43. Zur Y, Stokar S, Bendel P. An analysis of fast imaging sequences with steady-state transverse magnetization refocusing. Magn Reson Med 1988;6(2):175–193.

44. Constantinides CD, Atalar E, McVeigh ER. Signal-to-noise measurements in magnitude images from NMR phased arrays. Magn Reson Med 1997;38(5):852–857.

45. Buhk JH, Kallenberg K, Mohr A, Dechent P, Knauth M. Evaluation of angiographic computed tomography in the follow-up after endovascular treatment of cerebral aneurysms: a comparative study with DSA and TOF-MRA. Eur Radiol 2009;19(2): 430–436.

46. Buxton RB, Frank LR, Wong EC, Siewert B, Warach S, Edelman RR. A general kinetic model for quantitative perfusion imaging with arterial spin labeling. Magn Reson Med 1998;40(3):383–396.

47. Hadizadeh DR, von Falkenhausen M, Gieseke J, et al. Cerebral arteriovenous malformation: Spetzler-Martin classification at subsecond-temporal-resolution four-dimensional MR angiography compared with that at DSA. Radiology 2008;246(1):205–213.